Rapid Prediction of Damage to Struck and Striking Vessels in a Collision Event

Marie Lützen (PhD Student)**, Bo Cerup Simonsen** (Assistant Professor), **Preben Terndrup Pedersen** (Professor)

Abstract

This paper presents theory and application examples of a mathematical model for rapid prediction of damage to both the side structure of a struck vessel and the bow of a striking vessel in a collision event.
The geometry of the bow of the striking ship is idealised such that it can be described by only few parameters, still covering with sufficient accuracy almost all existing ship bows with and without bulbs.
The model for the internal mechanics of the struck ship side is based on a set of so-called super-elements. Each super-element represents an assembly of structural components and contains solutions for the structural behaviour of this assembly under deep collapse. By summing up the crushing force of each super-element, it is possible to determine the total contact load between the two involved ships.
A number of parameter studies are presented where the sensitivity of the damage to the loading conditions and striking positions are illustrated. Furthermore, the difference between longitudinal and transverse bow stiffening has been examined. Transversely stiffened bows are shown to be significantly softer than longitudinally stiffened bows.
Thirty collision events with five different striking vessels and six different struck vessels have been examined. The examples illustrate that the usual assumption of a rigid bow only holds true for certain categories of struck and striking vessels.

1 INTRODUCTION

Although continuous efforts are being made to prevent the occurrence of ship collision and grounding accidents it is certain that these accidents will continue to occur. With an ever-increasing societal demand for safety, it is of great interest to be able to predict the probability and outcome of these accidents.

Today ships have a built-in passive safety, which is mainly based on previous accidents, often triggered by single disasters. The requirements to subdivision of ships, for instance, are based on damages that were measured after accidents that occurred more than 30 years ago. This means, of course, that when new innovative ship designs are being introduced it can be very difficult – not to say impossible – to consistently use existing accident statistics and set up rational requirements to the passive safety. Furthermore, although it is known that the ship structure has large influence on the damages and consequences of an impact, the ship designer has no incentive today to optimise the so-called crashworthiness of the ship.

However, there is a trend in the marine sector towards rational risk analysis where more modern methods are being used to predict the probability, damage and consequence of various accidents. For example the International Maritime Organisation (IMO) has recently set up guidelines for use of formal safety assessment in the rule development process, [1]. This is a clear indication that the maritime society is working towards more rational safety regulation of individual ships instead of the generalised, prescriptive regulations that have evolved over the past 150 years.

One of the main challenges in a rational safety assessment is to determine the damages and consequences of a set of accident scenarios. Normally the total problem is divided into external dynamics (global ship motions) and internal mechanics (crushing of the structure). The external dynamics can be solved by numerical solution of the equations of motion or by an integrated approach where the conservation of energy, momentum and angular momentum during the impact is used to derive analytical expressions for the dissipated energy. The present paper uses the approach of the latter kind developed by Pedersen and Zhang [2]. Roll, pitch and heave motions are neglected.

The internal mechanics involved in ship collision and grounding accidents is complex involving deep collapse with large displacements and rotations, large plastic deformations, fracture and friction. These phenomena are difficult to quantify and the current techniques and procedures for damage prediction are not at a stage where naval architects can do crash analysis accurately and unambiguously. There are two classes of theoretical methods which can be used to predict the damage of a collision: the finite element method and simplified, analytical methods (often referred to as 'super-element methods'). Experiments are normally too costly to be used for other purposes than validation of theory.

Recent work has shown that the finite element method can be used to perform both ship collision and grounding analysis, see for example Kuroiwa [3], Kitamura [4] or Sano et al. [5]. Although problems of fracture have not yet been fully resolved, the solutions of a finite element analyses can be detailed and accurate. However, the finite element modelling requires a massive effort both in terms of modelling and computer power so for many practical problems it is prohibitively expensive (especially if stochastic simulation of a large number of accidents is required). A more course and therefore less complicated finite element method for collision analysis of double hull tankers has recently been presented by Paik et al. [6].

The other group of methods covers a range of procedures, which are sufficiently simple that they can be used by hand calculations. The most famous of these methods was proposed by Minorsky in 1959 [7]. The basic idea is that the absorbed energy is a simple linear function of the volume of deformed material. Several modifications have been proposed to widen the applicability or the accuracy of the method. Most recently Pedersen and Zhang [8] introduced parameters for the structural lay-out in a formula similar to Minorsky's.

At a more detailed level, many papers over the past have proposed fundamental, closed form solutions to various impact problems involving structural crushing and tearing deformation. For example Wierzbicki and Abramowich [9] and Amdahl, [10], developed several fundamental solutions, which may be used to estimate the energy absorption in axial crushing of plate intersections like X-forms, T-forms etc. Likewise other solutions are known for indentation into shell plating, crushing of a deck or a deep web girder etc. These special solutions – often referred to as super-element solutions – are known to predict the energy absorption quite accurately but at the same time, they only apply to very specific loading cases. This means, for example, that the solution for axial crushing of a T-form is accurate if the T-form is crushed axially, but if the loading direction is slightly different, the T-form solution may not work. The consequence of this limited applicability of each super-element is that if one wants to model a complex side structure which is being penetrated by a bow it is essential to be able to re-mesh, or re-discretize, the structure as the solution proceeds. The computer program *DAMAGE* [11], for analysis of grounding and collision events, is based on such an approach similar to the one used in this paper.

It is a common practice to assume that the bow of the striking ship does not deform during the impact.

Obviously, this assumption is very convenient for the analysis but at the same time it is known, that the assumption does not always hold true, see for example Lehman and Yu [12]. A major goal of the present paper is to investigate limits of validity for this assumption. Therefore, both the striking bow and the side of the struck ship are modelled by the super-element approach in the present analyses.

2 MODELLING OF INTERNAL MECHANICS IN SIDE STRUCTURE

This section describes how the resistance of the struck ship to the penetration of the striking ship is calculated. Here we shall first assume that the bow of the striking vessel is rigid during the penetration into the struck vessel.

2.1 Basic Idea: Super-Elements and Adaptive Discretization Scheme

The model for the internal mechanics is based on a set of so-called super-elements. Each super-element represents a structural component and contains solutions for the structural behaviour of this component during deep collapse.

Each super-element solution has the following characteristics

- The super-element solution describes accurately the complex, highly non-linear collapse behaviour of a large structural component (or assembly of components)
- The super-element solution is only applicable to a limited number of loading cases

The last point can easily be exemplified by a typical situation from a ship-ship collision. If the bow strikes in between two transverse web frames, it is possible to model the structural behaviour of the deck accurately by use of two different solutions. Before fracture is initiated, several models have been developed for the deck/girder crushing, see [13] and Figure 1. After initiation of fracture the solution for concertina tearing can be used, see [14] and [15]. However, after a certain penetration the bow may come into contact with the transverse bulkhead or frame. When this happens, the main resistance of the struck ship comes from the intersection between the transverse frame and the deck. Therefore it is more reasonable to switch to a modelling based on this particular case which is the so-called T-form super-element, Figure 2. The above example illustrates that use of super-element solutions calls for adaptive or successive discretization.

The present calculation procedure uses such adaptive discretization. The bow is incremented into the side of the struck ship. At each step the structure of the struck ship is discretized into super-elements and the contribution of each super-element is added to give the total resistance.

The super-element solutions used in the present calculation model are illustrated in Figures 1 and 2.

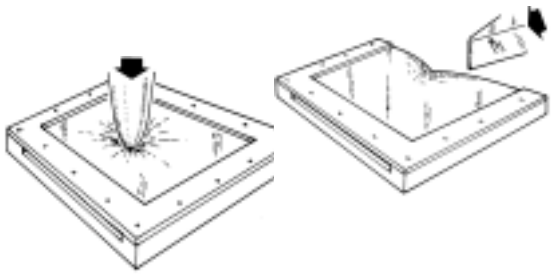

Figure 1. The Super-Elements used to model the resistance of membrane plates and the deck structure

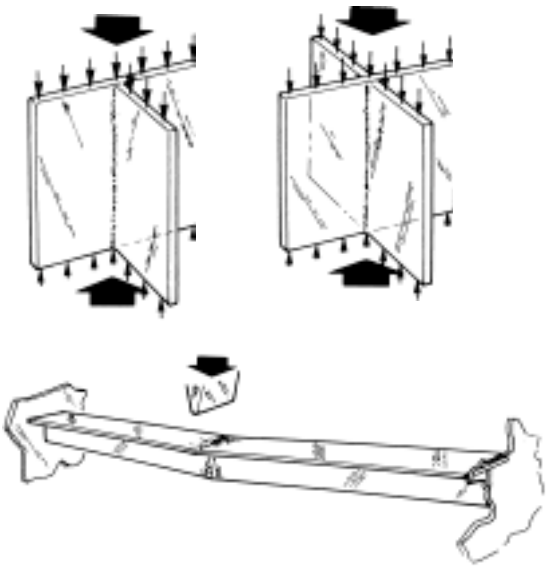

Figure 2. The Super-elements used to model beams, X- and T-elements

The super-elements are:

- Shell and inner side plating. A special non-linear plate element has been developed, which takes into account that the plate may be intact, or it may be fractured in the longitudinal direction, in the transverse direction or both directions. See Ref. [16]
- Deck and girder. When a deck or a girder is loaded by a point load, it will first collapse plastically with folds extending to the nearest boundaries. After a certain penetration, the plate will fracture at remote boundaries, and the plate will continue to fold up in

front of the bow like a concertina. See Refs. [13] and [17]

- Beam. This is the solution for a heavy beam loaded by a point load. The beam first fails by forming a mechanism of plastic hinges and then after a certain deformation it behaves like a plastic string. After fracture its resistance is zero. See Refs. [17] and [18]
- T-form intersections. For example the intersection between a transverse bulkhead and the weather deck can be modelled as a T-form. When the axial shortening becomes equal to the length of the T-form, the load drops to zero. See Refs. [10] and [19]
- X-form intersections. For example the intersection between a transverse bulkhead and a mid-deck can be modelled as a X-form. When the axial shortening becomes equal to the length of the T-form, the load drops to zero. See Refs. [10] and [19]

The considered structural elements are:

- Bottom
- Inner bottom
- Weather deck
- Shell plating
- Inner hull plating
- Mid decks
- Transverse bulkheads
- Longitudinal Bulkheads
- Floors
- Stringer decks
- Frames

The above structural elements may be equipped with vertical, longitudinal or transverse stiffeners.

2.2 Description of the Striking Bow

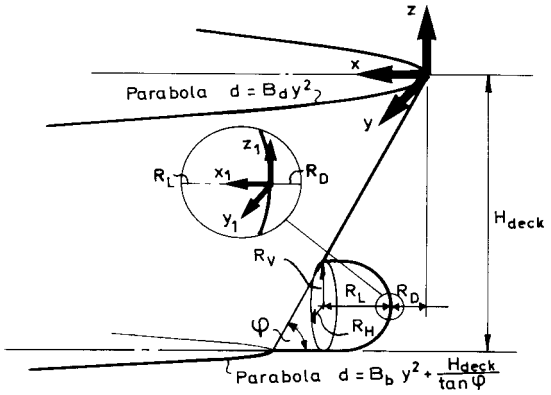

Figure 3. Assumed geometrical shape of the bow

The bulbous bow is divided into two parts, a conventional bow and a bulb.

The basic data for describing the assumed conventional bow is (se also Figure 3):

φ Stem angle
B Breadth of ship
H_{deck} Uppermost deck height
B_d,B_b Deck and bottom coefficients. The horizontal shape of the deck and bottom is assumed to be parabolic;

The bulb is assumed to have the form of an elliptic parabola. In a local co-ordinate system with origin in the bulb tip, the bulb is described as

$$\frac{x_1}{R_L} = \frac{y_1^2}{R_H^2} + \frac{z_1^2}{R_V^2}$$

where

R_L Length of bulb
R_V Vertical radius of bulb
R_H Horizontal radius of bulb

The distance between the bulb tip and the foremost part of the bow is denoted R_D.

3 MODELING OF THE MECHANICS OF BOW CRUSHING

3.1 Deformation of Longitudinally Stiffened Bow

A method for determination of impact loads as a function of deformation for bow collisions against rigid walls is developed by Pedersen et al. [20]. The method is based on a modification of Amdahl's method [10], which has been established on the basis of theoretical considerations of energy dissipated during plastic deformation of basic super elements such as angles, T-sections and cruciforms. The formula for the average crushing strength is given by

$$\sigma_c = 2.42\sigma_0 \left[\frac{n_{AT} t^2}{A}\right]^{0.67} \cdot \left[0.87 + 1.27 \frac{n_c + 0.31 n_T}{n_{AT}} \left(\frac{A}{(n_c + 0.31 n_T) t^2}\right)^{0.25}\right]^{0.67} \quad (1)$$

The total crushing load is found by multiplying with the associated cross-sectional area of the deformed steel material

$$F_c = \sigma_c A$$

where

σ_c average crushing strength of bow;
σ_0 flow stress;
t average plate thickness of cross-section under consideration;

A cross-sectional area of deformed steel material;
n_c number of cruciforms;
n_T number of T-sections;
n_{AT} number of angle- and T-sections

3.2 Deformation of Transversely Stiffened Bow

The method developed by Pedersen et al. [20] is by Lehmann and Yu [12] said not to be suitable for transversely stiffened bows. They developed a method based on a study of crushing of conical shell structures. The shell plating of the bulb is idealised as a series of short conical shells with different cone angles.
The average crushing load for each shell is given by

$$F_C = 2.09\sigma_0 t^2\left[\frac{2\pi R_i}{L}+\frac{L}{t}+(\pi+2\varphi)\tan\varphi+1\right] \qquad (2)$$

where
σ_0 ultimate strength of steel;
t plate thickness;
L frame spacing;
R_i effective radius;
φ conic angle
Internal elements such as decks and longitudinal bulkheads are treated as super elements, where the crushing strength is calculated using Eq. (1).

3.3 Comparison of Formulas for Bow Crushing

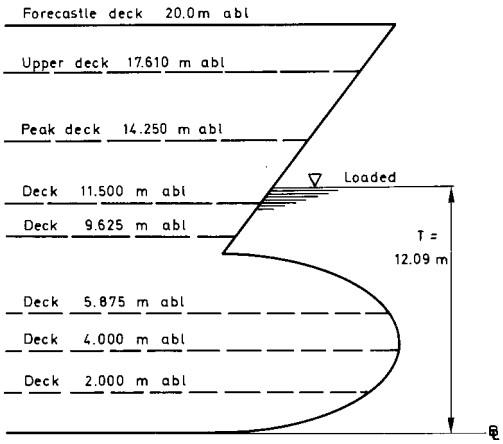

Figure 4. Bow geometry of a 51,800 DWT Bulk Carrier

The two equations, Eq. (1) and Eq. (2) are compared for a transversely stiffened bow. The crushing load is calculated for a 51,800 DWT bulk carrier. Main data and bow geometry can be found in Table 4, and the scantlings of the transversely stiffened bulb can be found in Table 1 and Figure 4. The forces calculated by the two equations are quite similar, as seen by a comparison of the force-deformation curves in Figure 5.

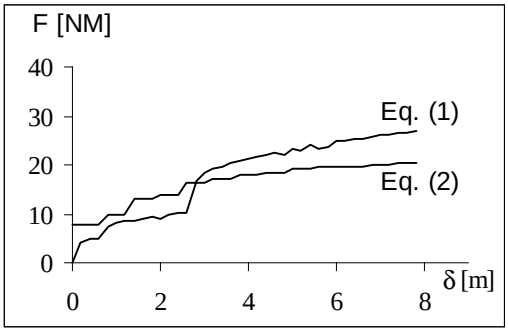

Figure 5. Comparison of Eq. (1) and Eq. (2). Crushing of the bulb of a 51,800 DWT Bulk Carrier (transversely stiffened) against a rigid wall

Table 1. Structural bow details of 51,800 DWT Bulk Carrier with transverse stiffened bow

Material:	
Yield Stress for Plates and Stiffeners	265.0 MPa
Bulb:	
Frame Spacing	610 mm
Shell Plate Thickness	13.5 mm
Stringer Deck Thickness H = 2.000 m H = 4.000 m H = 5.875 m	 8.0 mm 8.0 mm 8.0mm
Centreline Bulkhead Thickness	7.5 mm
Top of Bow:	
Shell Plate Thickness	13.5 mm
Forecastle Deck H = 20.000 m Thickness Stiffening: Long. Girders incl. CL Girder 400 X 120 X 11.5/23 Spacing 3000 mm	 9.5 mm
Upper Deck H = 17.610 m Thickness Stiffening: Long. Girders incl. CL Girder 400 X 120 X 11.5/23 Spacing 3000 mm	 10.0 mm
Peak Deck H = 14.250 m Thickness Stiffening: Long. Girders incl. CL Girder 400 X 120 X 11.5/23 Spacing 3000 mm Transverse Stiffening 230 X 9 Spacing 610 mm	 8.0 mm

Table cont. next page

Table 1. (Cont.) Structural bow details of 51,800 DWT Bulk Carrier with transverse stiffened bow

Stringer Deck Thickness H = 11.500 m H = 9.625 m Stiffening: Transverse Stiffening 230 X 9 Spacing 610 mm	 8.0 mm 8.0 mm
Centreline Bulkhead up to 14.250 m Thickness	 7.5 mm
Bottom:	
Height of Double Bottom	2.0 m
Bottom, Thickness	15.5 mm
Inner Bottom, Thickness	15.5 mm
Centreline Girder, Thickness	16.0 mm
Girders Spacing 3.0 m, Thickness	15.0 mm
Floors Spacing 610 mm, Thickness	13.5 mm

3.4 Deformation of Both Striking and Struck Vessel

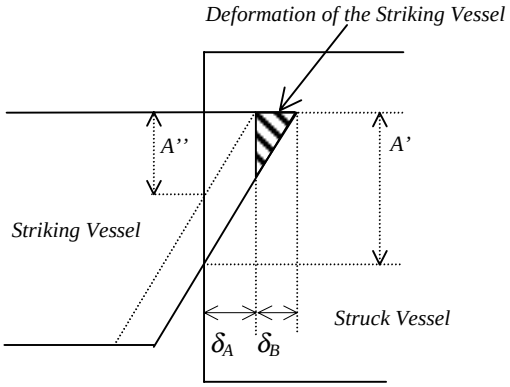

Figure 6. Deformation of vessels during collision. The A's relate to areas not lengths

The analysis of collision scenarios, where both the striking and the struck vessel can be damaged, is carried out in penetration steps. Only one of the involved vessels can be deformed in each step. By a comparison of the crushing forces for respectively the bow and the side, it can be determined which vessel deforms during the considered step.

Before calculation of the deformation of the two vessels the following calculations are carried out

1. Force-Penetration curve $F_{struck}(\delta_A)$ for the struck vessel, where the striking vessel is rigid
2. Force-Penetration curve $F_{striking}(\delta_B)$ for the striking vessel, where the struck vessel is rigid

If the striking vessel is equipped with a bulbous bow, the analysis of the crushing forces is separated into a bulb analysis and an analysis of the top of bow above the bulb.

A commonly used procedure for taking into account the deformation of the bow is to compare the two above mentioned force-penetration curves, $F_{struck}(\delta_A)$ and $F_{striking}(\delta_B)$, at each step. This approach, however, only includes a very limited level of interaction. In reality, the force-penetration curve for the side of the struck vessel is a function of the deformation of the bow, and vice versa. This stronger interaction is taken into account by comparing the forces F_A and F_B, which is determined as

Struck vessel $\quad F_A = F_{Struck}(\delta_A)\frac{A'}{A''}$

Striking vessel $\quad F_B = F_{Striking}(\delta_A + \delta_B)$

where

F_A force to crush the struck vessel;
F_B force to crush the striking vessel;
F_{struck} force from the force-penetration curve for struck vessel, where the striking vessel is rigid;
$F_{striking}$ force from the force-penetration curve for striking vessel, where the struck vessel is rigid;
δ_A penetration into the struck vessel;
δ_B deformation of the striking vessel;
A' cross-sectional area of the striking vessel taken at a distance of $\delta_A+\delta_B$ from bow or bulb tip;
A'' cross-sectional area of the striking vessel taken at a distance of δ_A from bow or bulb tip;

See also Figure 6.

The forces at the struck and the striking vessel F_A and F_B are compared

- If $F_A > F_B$
  Deformation of striking vessel, δ_B is increased
- If $F_B > F_A$
  Deformation of struck vessel, δ_A is increased

The reason for correcting the resistance of the struck vessel is, that if the bow is deformed, the resistance is approximately equal to the force at the side times the ratio between the areas. For a single hull vessel the correction will have nearly no influence, but for a double hull vessel, there will be some corrections when the bow penetrates the inner side, see Figure 6.

When the deformation patterns of the struck and the striking vessel are known, the total absorbed energy can be calculated and compared with the energy calculated by the external dynamics, see Pedersen and Zhang [2].

4 APPLICATION EXAMPLES

In order to investigate the sensitivity of collision analysis results, we shall in this section present numerical analysis of the effect of:

1. The local collision location relative to the web framing
2. The global longitudinal striking location along the hull girder
3. The vertical striking location, i.e. the influence of the loading condition of the involved vessels
4. Comparison of a transversely and a longitudinally stiffened bow
5. The effect of the crushing strength of the striking bow

For the first three sensitivity analyses two specific vessels have been chosen.

4.1 Crude Oil Carrier struck by Container Vessel

The struck vessel is a 105,400 DWT double hull crude oil carrier. The main data for this vessel is:

Length 234.0 m
Breadth 42.0 m
Depth 21.0 m
Draught 14.9 m
Mass 122,870 mt

A description of the scantlings may be found in Tables 2 and 3, see also Figures 7 and 8.

The striking vessel is a 40,000 DWT container vessel with high Baltic ice class (DnV ice class 1B). Main data and bow-geometry can be found in Table 4. The scantlings may be found in [20].

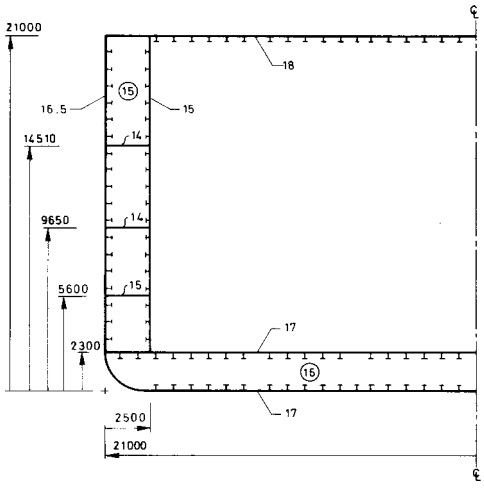

Figure 7. Scantlings of a 105,400 DWT Crude Oil Carrier, cargo hold section

Table 2. Structural data for cargo hold section, See also Figure 7

Material Yield Stress 310 MPa
Frame Spacing 3700 mm
Deck Stiffeners Longitudinal: 300 X 90 X 11/16 Spacing 830 mm Transverse : 1500 X 12.5 Spacing 3700 mm
Side and Inner Side Stiffeners All Longitudinal with Spacing 810 mm Between 0 and 5600 mm abl.: 400 X 100 X 13/18 Between 5600 and 9650 mm abl.: 400 X 100 X 11.5/16 Between 9650 and 14510 mm abl.: 300 X 100 X 12/17 Between 14510 and 21000 mm abl.:300 X 90 X 11/16
Bottom and Inner Bottom Longitudinal: 450 X 125 X 11.5/18 Spacing 830 mm
Transverse Bulkhead Thickness 15 mm Longitudinal Stiffeners : 450 X 125 X 11.5/18 Horizontal Stiffeners : H = 14510, 9560 and 5600 mm abl. 2000 X 150 X 12/12

Table 3. Structural data for engine section, See also Figure 8

Material Yield Stress 310 MPa
Frames 400 X 12 Spacing 800mm
Deck Stiffeners H = 9650 mm abl. Longitudinal: 700 X 150 X 11/15 Spacing 830 mm H = 14510 mm abl. Longitudinal: 700 X 150 X 11/15 Spacing 830 mm
Side Stiffeners Longitudinal: 250 X 12 Spacing 830 mm
Bottom and Inner Bottom Longitudinal: 300 X 90 X 13/17 Spacing 830 mm
Long. Bulkhead y=7000 mm Vertical Stiffening: 400 X 15 Spacing 800 mm
Long. Bulkhead y=12500 mm Longitudinal Stiffening: 200 X 11 Spacing 830 mm

When comparing forces for the struck vessel and the striking bow, it is found that only the struck vessel will deform. For this particular case the striking vessel can therefore be assumed to be rigid.

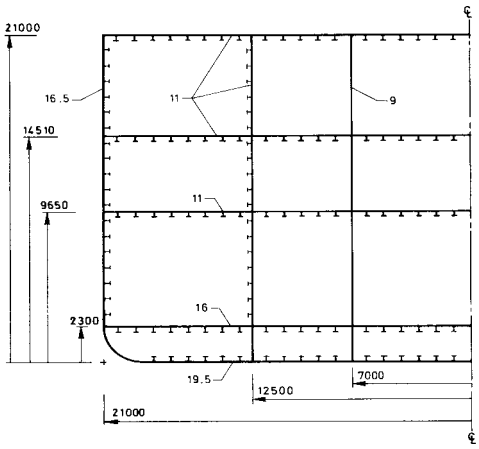

Figure 8. Scantlings of 105,400 DWT Crude Oil Tanker, engine section

4.1.1 Sensitivity to Longitudinal Striking Location (Local)

To determine the effect of either striking a transverse web frame or having the collision point between two web frames, we consider a right angle collision, where the struck vessel has zero speed. The striking vessel has a velocity of 3, 5 or 7 knots. Both vessels are fully loaded. The collision locations are placed in the tank at mid ship. Figure 9 shows the penetration into the struck vessel as a function of the striking location. Depicted in Figure 9 is also the plan view of the side structure of the double hull side of the tanker. The penetration pattern for the 5 and 7 knot collision speeds are similar. A decrease in penetration occurs, when the striking location is between two frames. The main reason for this decrease in penetration is that when the bow is between two frames, it will early come into contact with both frames. The case where the velocity of the striking vessel is three knots is different. The deepest penetration occurs if the striking location is between two frames. The main absorption of energy will in this case be in membrane plates as crushing elements are touched late in the process.

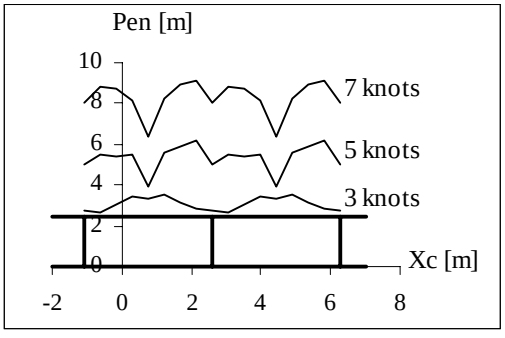

Figure 9. Penetration into a 105,400 DWT Crude Oil Carrier as a function of striking location (local)

A decrease in frame spacing or a striking vessel with a smaller deck coefficient B_d, will cause the curves to be more flat.

4.1.2 Sensitivity to Longitudinally Striking Location (Global)

We will now investigate whether it is important to model in detail the variation of the contact point along the length of the hull. Figure 10 shows the results of such an analysis. The penetration into the struck double hull crude oil tanker is plotted as a function of the striking location. The striking positions are in the centre of each cargo tank at a frame and in the centre of the engine room aft.

The collision is again a right angle collision, where the struck vessel has zero speed. The striking vessel has a velocity of 3, 5 or 7 knots. Both vessels are fully loaded.

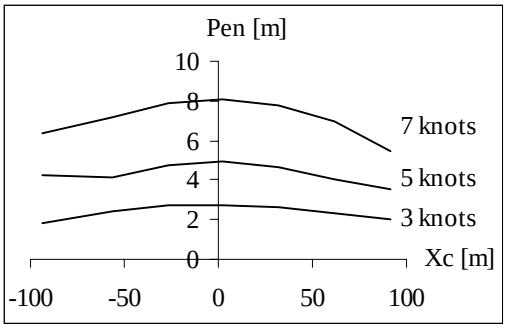

Figure 10. Penetration into struck vessel as a function of striking location(global)

The Figure shows the effect of the external dynamics i.e. most energy has to be absorbed around mid ships. In the aft part of the struck vessel, which is a single hull section in the engine region (Figure 8), there is a slight modification in the penetration pattern. For the 3 knots case, there will be a decrease in the penetration, which is due to the relatively thick mid decks in the engine section, and that only few crushing elements are touched in the hold region. In the 5 knots case the penetration will increase in the engine region. In this case many elements will be crushed in the hold section, whereas we still only have mid decks in the engine section. The penetration curve is flattening in the 7 knots case, where the bow will penetrate a longitudinal bulkhead in the engine section.

4.1.3 Sensitivity to the Vertical Striking Location

In order to analyse the importance of the vertical striking location in a collision, the same two vessels are considered, i.e. the striking 40,000 DWT container vessel and the 105,400 DWT crude oil carrier described above. Again the collision is a right angle collision with zero speed of the struck double hull tanker. The striking

container vessel has a velocity of 7 knots. The crude oil carrier is either fully loaded or in ballast, as these conditions are normal for tankers.

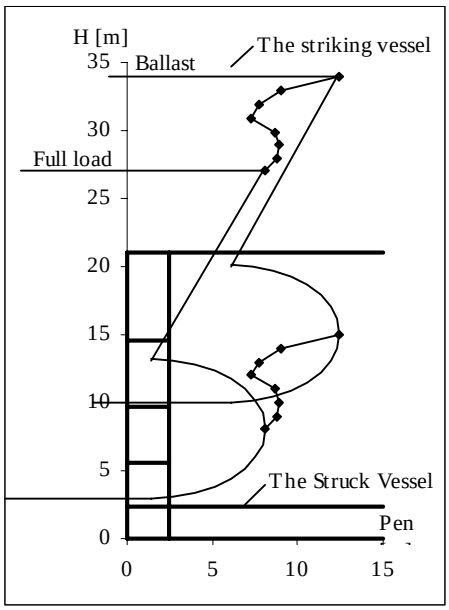

Figure 11. Penetration into struck vessel, struck vessel is fully loaded; varying draught of striking vessel

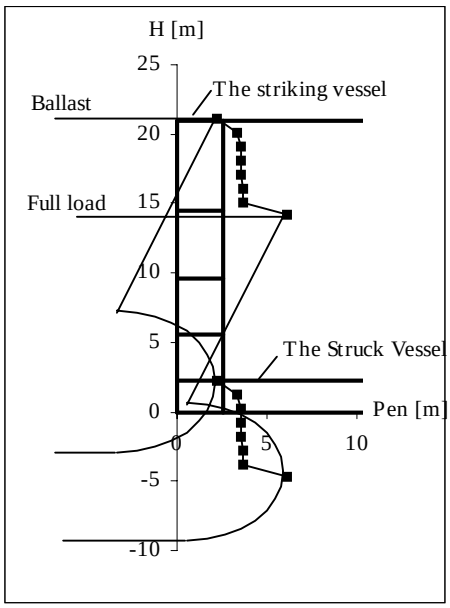

Figure 12. Penetration into struck vessel, struck vessel is in ballast; varying draught of striking vessel

The crude oil carrier has a displacement of 17,000 tons and a draught of 2.1 m in ballast.
The calculations show that the largest penetration occurs, when the crude oil carrier is fully loaded and the container vessel is in ballast. This is partly a result of the external dynamics and partly because the striking vessel only touches the upper part of the struck vessel. Figures 11 and 12 shows the envelopes of maximum penetration at varying draught of striking vessel (positions of bulb- and bow-tip are marked in the cross-section of the struck vessel). It is remarkable that the only situation, where the striking vessel does not penetrate the inner side of the struck ship, is, when both the crude oil carrier and the container vessel are in ballast, which is not a normal situation for a container vessel.
The large penetration is also remarkable, considering that the velocity, 7 knots, is close to the lowest manoeuvrable speed for the container vessel.

4.2 Comparison of Longitudinally and Transversely Stiffened Bow

Before a presentation of the effect of the crushing deformation of the bow of the striking vessel, we shall first consider the variation in bow strength for two different stiffened vessels. The two vessels that will be compared are a container vessel of 40,000 DWT with high ice class and a bulk carrier of 51,800 DWT.
The geometrical data for the two vessels are shown in Table 4, the scantling data for the container vessel can be found in [20] and the structural data for the bulk carrier can be found in Table 1 and Figure 4.

Table 4. Geometric bow-data. See also Figure 3

		Container	**Bulk Carrier**
DWT		40,000	51,800
Length	L_{pp}	211.50 m	205.25 m
Breadth	B	32.20 m	30.50 m
Depth	D	24.00 m	20.00 m
Draft	T	11.90 m	12.09 m
Displacement	Δ	54,000 t	70,000 t
Stem angle	φ	61.5^0	53.0^0
Deck coeff.	B_d	0.109 m^{-1}	0.147 m^{-1}
Bottom coeff.	B_b	20.000 m^{-1}	0.076 m^{-1}
Bulb:			
Length	R_L	7.50 m	8.50 m
Vertical axis	R_V	5.10 m	4.50 m
Horizontal axis	R_H	2.50 m	5.00 m
Bulb start	R_D	0.00 m	0.00 m

The two vessels are comparable in size and geometry, but the structural layout of the two bows is different.
The result is that the bow of the bulk carrier, which is transversely stiffened, shows a significantly lower resistance, as seen by comparison of the force-penetration curves in Figure 13.

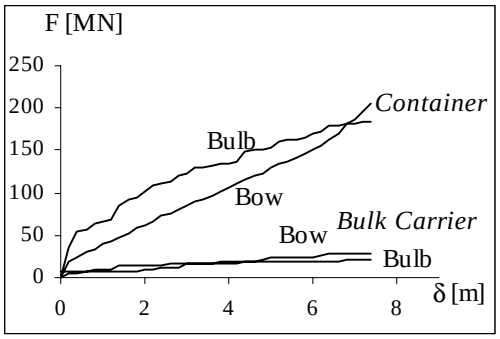

Figure 13. Calculated load deflection curve for the 40,000 DWT Container Vessel (longitudinally stiffened) and the 51,800 DWT Bulk Carrier (transversely stiffened)

4.3 Reduction in Penetration due to Bow Deformation

In the fifth sensitivity analysis we shall carry out a series of computer simulations of collisions involving 11 different ships in order to determine when the energy released for crushing is absorbed by the bow of the striking vessel or absorbed by the side structure of the struck vessel.

Five different striking vessels are considered:

1. 150,000 DWT bulk carrier
2. 40,000 DWT container vessel
3. 3,000 DWT general cargo vessel
4. 2,000 DWT tanker
5. 500 DWT coaster

The main particulars and geometry parameters of these five vessels are given in Tables 4, 5 and 6. The bow scantlings can be found in [20].

Table 5. Geometric bow-data

		Bulk Carrier	**Gen. Cargo**
DWT		150,000	3,000
Length	L_{PP}	274.00 m	78.00 m
Breadth	B	47.00 m	16.00 m
Depth	D	26.00 m	10.50 m
Draft	T	15.96 m	5.70 m
Displacement	Δ	174,850 t	4,594 t
Stem angle	φ	60.0^0	57.0^0
Deck coeff.	B_d	0.0741 m^{-1}	0.18 m^{-1}
Bottom coeff.	B_b	0.00299 m^{-1}	0.18 m^{-1}
Bulb:			
Length	R_L	7.50 m	2.90 m
Vertical axis	R_V	5.90 m	2.48 m
Horizontal axis	R_H	8.50 m	1.36 m
Bulb start	R_D	0.70 m	0.70 m

The present analysis is based on striking vessels with relatively strong bow structures. Since most ships have bulbous bows, and since bulbous bows are known to exert high collision resistance all the ships are analysed with bulbous bows. In order to get upper bounds for the local bow collision loads the scantlings given in Pedersen et al. [20] were taken such, that the vessels could obtain a Baltic ice class (DnV ice class 1B). To get sufficient ice strength the bulbous bows at all five vessels are constructed with longitudinal stiffeners in decks, longitudinal bulkheads and outer shells whereas for ease of construction, ships without ice strengthening normally have a transverse stiffening system such as the bulk carrier bow described in Section 3.3.

Table 6. Geometric bow-data

		Tanker	**Coaster**
DWT		2,000	500
Length	L_{PP}	69.00 m	41.00 m
Breadth	B	12.30 m	9.00 m
Depth	D	8.60 m	6.40 m
Draft	T	4.75 m	3.34 m
Displacement	Δ	3,016 t	886 t
Stem angle	φ	62.5^0	59.0^0
Deck coeff.	B_d	0.286 m^{-1}	0.573 m^{-1}
Bottom coeff.	B_b	0.286 m^{-1}	0.573 m^{-1}
Bulb:			
Length	R_L	2.20 m	1.80 m
Vertical axis	R_V	1.90 m	1.41 m
Horizontal axis	R_H	1.10 m	0.83 m
Bulb start	R_D	0.30 m	0.35 m

Six different struck vessels are considered. The struck vessels are separated into two groups, tankers and RoRo vessels.

The tanker group consists of three vessels with lengths of 103 m, 198 m and 317 m. The vessel of 103 m is transversely stiffened, whereas the two other vessels are longitudinally stiffened. The main particulars and the most important structure can be seen in Table 7.

The three RoRo vessels are ships examined by Det Norske Veritas [21] and Germanisher Lloyd [16] during the Joint North-West European Research Project.

Main Particulars for three RoRo Vessels

	RoRo 1	RoRo 2	RoRo 3
Length [m]	58.0	150.0	180.0
Breadth [m]	13.0	27.0	31.5
Depth [m]	9.7	19.4	21.1
Draught [m]	3.5	6.0	7.0
Mass [mt]	1,600	15,800	27,000

The scantlings can be found in Refs. [16] and [21].

Also for this analysis the collision is a right angle collision, where the struck vessel has zero speed. The striking vessel has a velocity of 4.0 m/s. The striking position is in all cases at the frame nearest mid ship at the struck vessel.

Table 7. Main particulars and structural data for three single hull tankers. Tanker 1 is transversely stiffened whereas Tanker 2 and 3 are longitudinally stiffened

	Tanker 1	Tanker 2	Tanker 3
Length [m]	103.0	198.0	317.0
Breadth [m]	15.5	29.9	56.6
Depth [m]	6.9	14.9	31.5
Draught [m]	5.8	11.1	22.5
Mass [mt]	7,400	52,400	330,300
Material			
Yield stress[MPa]	250	250	250
Plate thickness [mm]			
Shell Plate	14	19.5	20
Bottom Plate	12	15	20
Deck Plate	14	19.5	20
Web frames			
Spacing [mm]	2900	3025	5400
Thickness [mm]	14	15	14
Depth [mm]	660	1000	3200
Floors			
Spacing [mm]	2900	3025	5400
Thickness [mm]	10	11.5	15
Depth [mm]	885	1450	3200
Stiffeners side and bottom			
Web thickness [mm]	10	12	15
Web depth [mm]	200	280	600
Flange thickness[mm]	10	15	15
Flange width [mm]	50	100	160
Spacing [mm]	720	760	950

Table 8 shows the penetration into the struck vessel, when the striking vessel is assumed to be rigid. The Table shows to a great extend the effect of the external dynamics, i.e. the penetration is increased, when the struck vessel has a larger mass, but there are exceptions. The penetration of the container vessel into the large tanker of 317 m is smaller than the penetration into the tanker of 198 m, which is due to the difference in height of the two tankers. The top of the large tanker will be crushed earlier than the medium tanker, which means the struck vessel will absorb more energy. For the smaller vessels, i.e. the general cargo vessel, the tanker and the coaster impacting the smallest tanker, and the coaster impacting the smallest RoRo vessel, we see the effect of a weak shell plate penetrated by slender vessels, where only a few frames are touched.

Table 9 shows the calculated actual penetration and Figures 14 and 15 show the reduction of the penetration into the struck vessel, when the actual strength of the bow is considered. We see a large reduction in the penetration for the three smaller striking vessels, whereas the bow of the ice strengthened bulk carrier and the container vessel does not deform.

Table 8. Penetration into struck vessel, where striking vessel is considered rigid, all numbers in meter

Striking Vessel / Struck Vessel	Bulk Carrier 150,000 DWT	Container Vessel 40,000 DWT	General Cargo 3,000 DWT	Tanker 2,000 DWT	Coaster 500 DWT
Tanker L = 103m	4.56	7.87	4.30	3.03	1.63
Tanker L=198m	16.10	19.31	2.30	1.50	0.70
Tanker L=317m	*	10.98	3.50	2.10	0.80
RoRo L=58m	3.32	3.00	2.40	2.00	1.50
RoRo L=150m	8.60	7.40	3.60	2.10	1.00
RoRo L=180m	9.00	8.20	3.70	2.30	1.20

** The bulk carrier penetrates the whole breadth of the tanker*

Table 9. Actual penetration into struck vessel, all numbers in meter

Striking Vessel / Struck Vessel	Bulk Carrier 150,000 DWT	Container Vessel 40,000 DWT	General Cargo 3,000 DWT	Tanker 2,000 DWT	Coaster 500 DWT
Tanker L = 103m	4.56	7.87	4.30	2.83	0.10
Tanker L=198m	16.10	19.31	1.30	0.30	0.20
Tanker L=317m	*	10.98	1.70	0.10	0.10
RoRo L=58m	3.32	3.00	2.40	0.10	0.20
RoRo L=150m	8.60	7.40	2.80	1.80	0.50
RoRo L=180m	9.00	8.20	3.60	1.90	0.40

The big reduction in penetration for the 2,000 DWT tanker striking the smallest RoRo vessel is partly due to a relatively weak bow, where the forepart deforms before it penetrates rigid into the side of the struck vessel, and partly due to the external dynamics. We see the same situation for the coaster impacting the small RoRo vessel.

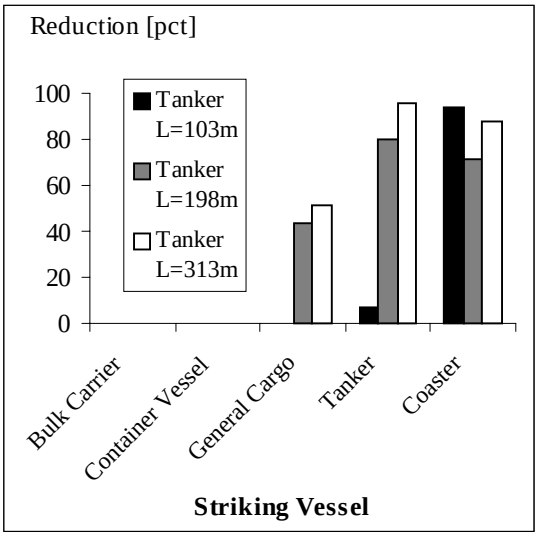

Figure 14. Reduction in penetration into struck vessel due to bow crushing

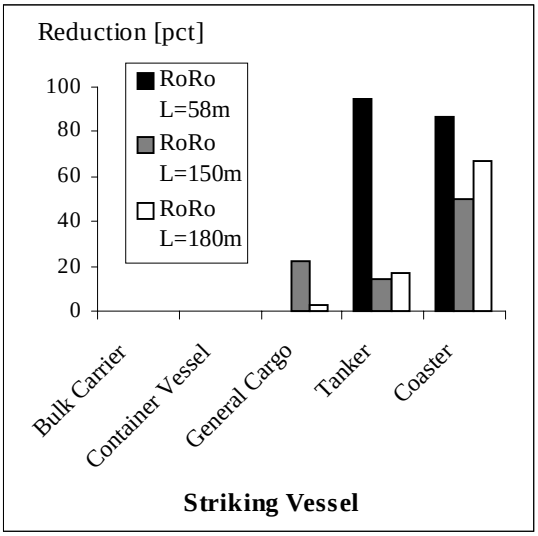

Figure 15. Reduction in penetration into struck vessel due to the bow crushing

Table 10 shows the energy absorbed in the striking bow as percentage of the total energy to be absorbed. Here again we see the effect of the external dynamics, and the relatively weak bows of the tanker and the coaster.

Table 10. Energy absorbed in the striking bow as percentage of the total energy

Struck Vessel \ Striking Vessel	Bulk Carrier 150,000 DWT	Container Vessel 40,000 DWT	General Cargo 3,000 DWT	Tanker 2,000 DWT	Coaster 500 DWT
Tanker L = 103m	0	0	0	24	97
Tanker L=198m	0	0	36	95	89
Tanker L=317m	0	0	52	99	94
RoRo L=58m	0	0	0	98	91
RoRo L=150m	0	0	20	48	82
RoRo L=180m	0	0	0.4	46	86

5 FUTURE WORK

The following list contains a number of items that would enhance the performance and reliability of the collision and deformation model

- Validation of calculation procedure, when both structure and indentor are deformed during the collision
- Further development for modelling of shell plating. As the shell plating absorbs a significant part of the energy, it is essential to model this component particularly accurately. It is necessary to revisit the theories for both resistance and fracture initiation and propagation
- Extent of deformation. The present model assumes the deformation extends from indentor to the nearest boundaries, and structural elements are not deformed before they are touched by the striking bow. This assumption works quite well for conventional ships, but for a double hull vessel, the inner side may deform, before the bow is in contact with the inner plating
- The deformation of bulkheads are defined as plate crushing, which works well if the load from the bow is a right angle impact, but if the bulkhead is inclined loaded large membrane forces must be found in the plate

- The vertical and the longitudinal extend of the damage must be further examined. The extend of damage at struck vessel indicates the amount of damaged watertight compartments, specially when both the striking and the struck vessel have velocity, the damage length can be significant extended

6 CONCLUSION

This paper has described basic principles and application examples for a collision model, where damage to the struck and striking vessels can be predicted. The theoretical model for the structural mechanics is based on a set of super-element solutions and an adaptive discretization procedure of ship side and bow.

Five parameter studies are presented. In three studies the striking vessel is assumed to be rigid. The sensitivity to longitudinal striking location is examined in two studies; one to show the local variation of crushing strength and one to show the global variation along the hull. The local analysis for the striking location shows that the deformation patterns depend on the distance between web frames, breadth of striking vessel and the penetration depth. The global analysis mostly shows the effect of the external dynamics. This means that the global variation of strength along the hull is quite limited. In the aft part of the vessel, where the engine room is situated, there is a slight modification to the penetration pattern but not significant. The last example for calculation with a rigid bow shows the sensitivity to the vertical striking location, i.e. the influence of the loading condition of the involved vessels; this example again shows both the effect of the external dynamics and the internal mechanics. The maximum penetration occurs when the struck ship is fully loaded and the striking vessel is in ballast. The minimum penetration occurs when both vessels are in ballast.

The crushing resistance of a longitudinally and a transversely stiffened bow of two ships of similar size are compared. The calculation shows a significantly lower resistance of the transversely stiffened bow.

Finally a series of 30 collision scenarios involving 11 ships are presented. Five striking vessels and six struck vessels of different types and lengths are used in the example. All striking vessels are longitudinally stiffened, i.e. they represent the ships with the strongest bows. Still, the analysis shows large bow deformation of smaller vessels. However, the bows of ice strengthened larger vessels can be assumed to be rigid.

REFERENCES

[1] Interim Guidelines for Approval of Alternative Methods of Design and Construction of Oil Tankers under Regulation 13F(5) of Annex I of MARPOL 73/78
Resolution MEPC. 66(37), Adopted September 14, 1995

[2] Pedersen P.T, and Zhang S.
On impact mechanics in ship collisions
Marine Structures No. 11, pp. 429-449, 1998

[3] Kuroiwa T.
Numerical Simulation of actual collision and grounding accidents
Proc. Of Int. Conference on Design and Methodologies for Collisions and Grounding Protection of Ships, San Francisco, California, 1996

[4] Kitamura, O.
Comparative study on collision resistance of side structure
Proc. of Int. Conference on Designs and Methodologies for Collision and Grounding Protection of Ships, San Francisco, 1996, paper 9-1. Also Marine Technology, Vol. 34, No. 4, pp. 293-308, Oct. 1997.

[5] Sano A., Muragishi O., Yoshikawa, T., Murakami, A. and Motoi, T.
Strength analysis of a new double hull structure for VLCC in collision
Proc. of Int. Conference on Designs and Methodologies for Collision and Grounding Protection of Ships, San Francisco, 1996, paper 8-1.

[6] Paik, J.K., Chung Y.C., Choe I.H., Thayamballi A.K., Pedersen P.T. and Wang G.
On Rational Design of Double Hull Tanker Structures against Collision
SNAME Annual Meeting, Paper No. 14, 1999

[7] Minorsky V.U.
An Analysis of Ship Collisions with Reference to Protection of Nuclear Power Ships
J. of Ship Research, Vol. 3, No. 2, pp. 1-4. 1959

[8] Pedersen P.T. and Zhang S.
Absorbed energy in collision and grounding
Department of Naval Architecture and Offshore Engineering, Technical University of Denmark, 1999
To be published in Journal of Ship Research 2000

[9] Wierzbicki T. and Abramowicz W.
On the Crushing Mechanics of Thin-walled Structures
Journal of Applied Mechanics, Vol. 50, 1983.

[10] Amdahl J.
Energy Absorption in Ship-Platform Impacts
Dr. Ing. Thesis, Report No. UR-83-34, The Norwegian Institute of Technology, Trondheim, 1983

[11] Little P., Pippenger D. and Simonsen B.C.
Development of a Computational Model for Predicting Damage to Tankers
Proc. Of Int. Conference on Design and Methodologies for Collisions and Grounding Protection of Ships, San Francisco, California, 1996

[12] Lehmann E. and Yu X.
Progressive Folding of Bulbous Bows
The Sixth International Symposium on Practical Design of Ships and Mobile Units (PRADS), September, 1995

[13] Wierzbicki T. and Simonsen B. C.
Global Structural Model of Bow Indentation into Ship Side
MIT Program on Rupture Analysis of Oil Tankers in Side Collision, 1996

[14] Amdahl J. and Kavlie D.
Experimental and Numerical Simulation of Double Hull Stranding
DNV-MIT Workshop on Mechanics of Ship Collision and Grounding, DNV Høvik, Oslo, September, 1992

[15] Wierzbicki T.
Concertina Tearing of Metal Plates
Int. J. Solids Structures, Vol. 32, No. 19, pp. 2923-2943, 1995

[16] Scharrer M.
Safety of Passenger/RoRo Vessels: Analysis of Collision Energies and Hole Sizes
Joint North-West European Research Project
Report by: Germanisher Lloyd, No. FI 96.099

[17] Simonsen B.C. and Ocakli H.
Experiment and Theory on Deck and Girder Crushing
Thin-walled Structures, Vol. 34, pp. 195-216, 1999

[18] Jones N.
Structural Impact
Cambridge University Press 1989

[19] Kierkegaard H.
Ship Collisions with Icebergs
Ph.D Thesis, Department of Naval Architecture and Offshore Engineering, Technical University of Denmark, 1993

[20] Pedersen P.T., Valsgaard S., Olsen D. and Spangenberg S.
Ship Impacts: Bow Collisions
Int. J. of Impact Engineering, Vol. 13, No.2, pp. 163-187, 1993

[21] Hysing T.
Safety of Passenger/RoRo Vessels: Damage and Penetration Analysis
Joint North-West European Research Project
Report by: Det Norske Veritas, No. 95-0419, 1995

Discussion